Developmental Cell, Vol. 7, 217–228, August, 2004, Copyright ©2004 by Cell Press

$EspF_U$ Is a Translocated EHEC Effector that Interacts with Tir and N-WASP and Promotes Nck-Independent Actin Assembly

Kenneth G. Campellone, Douglas Robbins, and John M. Leong*
Department of Molecular Genetics and Microbiology
University of Massachusetts Medical School
55 Lake Avenue North
Worcester, Massachusetts 01655

Summary

Several microbial pathogens including enteropathogenic *E. coli* (EPEC) exploit mammalian tyrosine-kinase signaling cascades to recruit Nck adaptor proteins and activate N-WASP-Arp2/3-mediated actin assembly. To promote localized actin "pedestal formation," EPEC translocates the bacterial effector protein Tir into the plasma membrane, where it is tyrosine-phosphorylated and binds Nck. Enterohemorrhagic *E. coli* (EHEC) also generates Tir-dependent pedestals, but in the absence of phosphotyrosines and Nck recruitment. To identify additional EHEC effectors that stimulate phosphotyrosine-independent actin assembly, we systematically generated EHEC mutants containing specific deletions in putative pathogenicity-islands. Among 0.33 Mb of deleted sequences, only one ORF was critical for pedestal formation. It lies within prophage-U, and encodes a protein similar to the known effector EspF. This proline-rich protein, $EspF_U$, is the only EHEC effector of actin assembly absent from EPEC. Whereas EHEC Tir cannot efficiently recruit N-WASP or trigger actin polymerization, $EspF_U$ associates with Tir, binds N-WASP, and potently stimulates Nck-independent actin assembly.

Introduction

Enteropathogenic *Escherichia coli* (EPEC) and enterohemorrhagic *E. coli* (EHEC) are closely related human pathogens that generate attaching and effacing (AE) lesions in order to colonize the intestine, damage the epithelium, and promote diarrheal illnesses (Donnenberg and Whittam, 2001; Nataro and Kaper, 1998). These lesions are characterized by a localized replacement of microvilli with organized filamentous (F-)actin "pedestals" beneath intimately adherent bacteria (Campellone and Leong, 2003; Celli et al., 2000; Frankel et al., 1998). The reproduction of pedestal formation on cultured mammalian cells provides an experimental system for dissecting both the signaling mechanisms that regulate actin assembly beneath the plasma membrane and the role that these processes play in *E. coli* pathogenesis.

In order to stimulate localized actin assembly, EPEC and EHEC utilize a type III secretion system that translocates effector proteins from the bacterium into the mammalian cell. The genes encoding this type III secretory apparatus are contained within a chromosomal pathogenicity island called the locus of enterocyte effacement (LEE), and the proteins that comprise these structures are generally greater than 95% identical between EPEC and EHEC (Perna et al., 1998). In contrast to the highly homologous secretion machinery, the sequences of LEE-encoded effectors that are transported by the type III systems, the *E. coli* secreted proteins (Esps), are less conserved (Perna et al., 1998).

The most divergent of the Esps is the translocated intimin receptor, Tir (EspE), which is only 58% identical between EPEC and EHEC, yet is critical for the formation of actin pedestals by each pathogen (DeVinney et al., 1999; Kenny et al., 1997). Remarkably, Tir is delivered into the mammalian plasma membrane where it adopts a hairpin loop conformation and serves as a receptor for the bacterial surface adhesin intimin (Deibel et al., 1998; Kenny et al., 1997). The binding of intimin to the central extracellular domain of Tir promotes clustering of the N- and C-terminal cytoplasmic regions and initiates localized actin assembly beneath the plasma membrane (Campellone et al., 2004). As a result of the fact that EPEC generates pedestals on cultured cells more rapidly and at a higher frequency than EHEC (Cantey and Moseley, 1991; Deibel et al., 1998), and because it is less hazardous to laboratory personnel (Donnenberg and Whittam, 2001), EPEC has been preferentially used in studies designed at elucidating mechanisms of actin assembly.

For EPEC, clustering of just the C terminus of Tir, even in the absence of all other effectors, triggers actin pedestal formation (Campellone et al., 2004). Within the host cell, this domain of EPEC Tir is phosphorylated on tyrosine 474 (Y474) (Kenny, 1999), a residue critical for binding the SH2 domains of the mammalian adaptor proteins Nck1 and Nck2 (hereafter referred to as Nck) (Campellone et al., 2002; Gruenheid et al., 2001). The importance of this interaction is highlighted by the observation that recruitment of Nck by Tir is both necessary and sufficient to initiate localized actin assembly (Campellone et al., 2002, 2004; Gruenheid et al., 2001). By stimulating Nck-mediated signaling cascades, EPEC recruits and activates N-WASP, a key regulator of the Arp2/3 actin-nucleating machinery (Higgs and Pollard, 2001; Rohatgi et al., 2001; Welch and Mullins, 2002) that is required for pedestal formation (Lommel et al., 2001).

In contrast to EPEC Tir, the EHEC Tir molecule contains neither a residue corresponding to Y474 nor any other detectable phosphotyrosines (Deibel et al., 1998; DeVinney et al., 1999). Consistent with these observations, EHEC does not recruit Nck to sites of adherence (Campellone et al., 2002) and is capable of generating pedestals on Nck-deficient cells (Gruenheid et al., 2001). In spite of the fact that its Tir protein does not bind Nck, EHEC recruits N-WASP (Goosney et al., 2001) and requires N-WASP for efficient pedestal formation (Lommel et al., 2004), suggesting that EHEC utilizes a distinct mechanism to activate N-WASP and stimulate actin polymerization.

In order to facilitate studies on EHEC-mediated actin assembly, several laboratories have engineered EPEC strains to express EHEC Tir instead of EPEC Tir. Surprisingly, these strains do not efficiently generate actin

*Correspondence: john.leong@umassmed.edu

Table 1. Cryptic Prophage U Is Critical for Actin Pedestal Formation by EHEC

O157-Island[a]	O-Island Description	Deleted Nucleotides	Deletion Size	Deleted EHEC ORFs	Actin Pedestal Formation[b]
Nonmutagenized EHEC					
NONE	Wild-type EHEC	NONE	NONE	0	+
Deletions within the Locus of Enterocyte Effacement (LEE)					
OI-148A (partial)	EHEC Type Three Apparatus #1 (ETTA1) Structural Proteins	4,677,931–4,686,861	8.9 kb	15	−
OI-148B (partial)	Translocated intimin receptor (Tir/EspE)	4,668,961–4,670,521	1.6 kb	1	−
Deletions outside of the LEE					
OI-7	Putative Macrophage Toxin	240,937–275,501	34.6 kb	29	+
OI-8	Cryptic Prophage (CP)-933H; CP-933I	304,283–329,948	25.7 kb	34	+
OI-10-13	EaeH Putative Adhesin	345,397–367,118	21.7 kb	12	+
OI-14-15	Putative Adhesin	367,178–383,667	16.5 kb	11	+
OI-36 (partial)	CP-933K	898,093–930,891	32.8 kb	35	+
OI-44 (partial)	CP-933M	1,273,361–1,282,639	9.3 kb	15	+
OI-50	CP-933N; SopA-like Protein; YopM-like Protein	1,628,193–1,673,449	45.3 kb	58	+
OI-52 (partial)	CP-933X	1,744,969–1,755,067	10.1 kb	13	+
OI-79	CP-933U; $EspF_U$	2,743,081–2,782,196	39.1 kb	46	−
OI-80	Putative Invasin	2,788,634–2,799,118	10.5 kb	4	+
OI-115	EHEC Type Three Apparatus #2 (ETTA2) Structural Proteins	3,784,516–3,805,333	20.8 kb	27	+
OI-122	Enterotoxin; Cytotoxin	3,920,980–3,942,164	21.2 kb	25	+
OI-144	Putative Adhesin	4,587,515–4,592,805	5.3 kb	2	+
OI-148C (partial)	CP-933L	4,651,372–4,657,314	5.9 kb	10	+
OI-172 (partial)	unknown	5,384,041–5,403,508	19.5 kb	13	+

[a] O157-specific genomic islands that are present within EHEC strain EDL933 and are not found in *E. coli* K-12 strain MG1655 are numbered according to Perna et al. (2001).

[b] HeLa cells infected with wild type EHEC or EHEC O-island mutants were quantitated for actin pedestal formation, as determined by intense F-actin staining beneath bound bacteria. Cells containing pedestals beneath at least 50% of associated bacteria were scored as positive (+); cells containing pedestals beneath less than 50% of associated bacteria were scored as negative (−). All mutants classified as positive formed pedestals at frequencies similar to wild type EHEC. Two independently derived strains were generated for each targeted O-island, and each strain yielded similar pedestal formation efficiencies in at least three separate experiments.

pedestals (Campellone et al., 2002; DeVinney et al., 2001; Kenny, 2001), implying that EHEC Tir by itself is not sufficient to initiate actin polymerization. However, the ability to form pedestals can be restored to these EPEC bacteria by coinfecting cells with an EHEC strain that retains a functional type III secretion system (DeVinney et al., 2001), suggesting that EHEC may require translocated effectors in addition to Tir, that are absent from EPEC, to promote N-WASP activation and localized actin assembly.

Since each of the 41 open reading frames (ORFs) within the EHEC LEE has a homologous counterpart in the EPEC LEE, it seems likely that any additional EHEC effectors required for pedestal formation are encoded elsewhere in the chromosome. This suggestion is supported by the finding that a cloned EPEC LEE allows nonpathogenic K-12 strains of *E. coli* to generate actin pedestals (McDaniel and Kaper, 1997), while a cloned EHEC LEE does not (Elliott et al., 1999). Aside from its LEE element, the prototype O157:H7 EHEC strain, EDL933, contains nearly 1400 genes distributed in 176 O157-specific islands (O-islands) that are not present in *E. coli* K-12 (Perna et al., 2001). While novel effectors required for pedestal formation may lie within these EHEC-specific sequences, they are apparently difficult to identify, since none have been uncovered in numerous genetic and proteomic screens that have been performed since EHEC was initially observed to form pedestals in the absence of tyrosine phosphorylation (Ismaili et al., 1995).

To identify non-LEE-encoded effectors that are required for localized actin assembly, we utilized the bacteriophage-λ recombination system (Murphy and Campellone, 2003) to generate specific deletions of 19 large EHEC O-islands. Among the 335 LEE-independent ORFs that were eliminated in this Red-assisted-pathogenicity-island-deletion (RAPID) screen, only one was critical for pedestal formation. It is found within a cryptic prophage (CP) termed 933U, and encodes a protein similar to the LEE-derived effector EspF. Despite the fact that its gene is located outside the LEE, this proline-rich effector, designated $EspF_U$, is delivered into mammalian cells by the LEE-encoded type III apparatus. $EspF_U$ allows an EPEC strain that expresses EHEC Tir to form pedestals, indicating that it is the only essential EHEC-specific effector of actin assembly. Whereas EHEC Tir by itself does not efficiently recruit N-WASP or trigger actin polymerization, $EspF_U$ interacts with both Tir and N-WASP and circumvents a need for Nck adaptors during actin pedestal formation.

Results

A Red-Assisted-Pathogenicity-Island-Deletion Screen Reveals a Second Chromosomal Locus Critical for Actin Pedestal Formation by EHEC

To identify additional EHEC genes required for actin pedestal formation, we utilized the λ-Red chromosome engineering system, used extensively in K-12 strains of

E. coli (Court et al., 2002), to generate precise deletions throughout the O157:H7 genome. Nineteen EHEC-specific islands ranging from 5–45 kb in length were targeted for complete or partial removal (Table 1). These large islands contained ORFs with annotations suggesting roles in pathogenesis (Perna et al., 2001), or prophage-like elements, which are known to encode virulence-associated proteins in many pathogens, including EHEC (Wagner and Waldor, 2002). The deleted islands comprised 0.33 Mb of sequence encompassing 350 EHEC-specific open reading frames, 335 of which were outside of the LEE (Table 1).

To determine which of the mutated EHEC strains generated in this RAPID screen retained the ability to generate actin pedestals, HeLa epithelial cells were infected with these bacteria, stained for F-actin, and examined microscopically. As previously reported (DeVinney et al., 1999), strains lacking either the LEE-encoded EHEC type three apparatus (ETTA1) or the Tir effector were incapable of forming pedestals on cultured cells (Table 1). In contrast, all but one of the strains containing deletions of the non-LEE islands generated pedestals at efficiencies similar to wild-type EHEC (Table 1). Only the mutant lacking O-Island #79, which harbors a cryptic prophage designated CP-933U (CP_U), was apparently defective at stimulating actin assembly (Table 1).

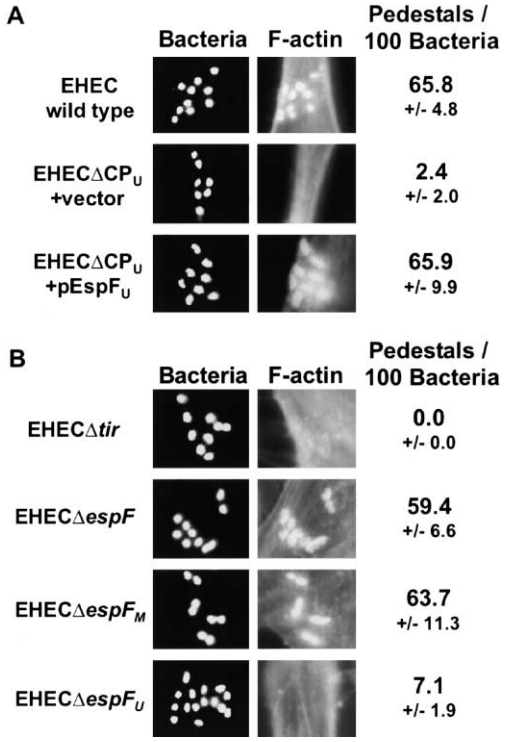

Figure 1. EHEC $espF_U$ Is Required for Efficient Actin Pedestal Formation

(A) HeLa cells were infected either with wild-type EHEC or with EHECΔCP_U harboring a control plasmid or a plasmid containing $espF_U$. Infected cells were treated with DAPI to identify bacteria and with phalloidin to stain F-actin. Pedestal formation efficiencies were quantitated by measuring the % of cell-associated bacteria that were also associated with intense F-actin staining. Data are the means (±SD) of three separate experiments.

(B) HeLa cells infected with the depicted EHEC strains were examined as described in (A).

EHEC $espF_U$ Is Required for Efficient Actin Pedestal Formation

CP_U contains 46 open reading frames (Perna et al., 2001); one of these, ORF Z3072, is predicted to encode a 384-residue protein that is 35% similar to EspF, a translocated effector encoded within the LEE elements of both EHEC and EPEC (McNamara et al., 2001). Since its ORF resides within cryptic prophage U, we termed this gene $espF_U$. To test whether the inability of EHECΔCP_U to form pedestals was due to the absence of $espF_U$, this strain was transformed with a plasmid containing $espF_U$ and examined for pedestal formation. While approximately 65% of wild-type EHEC bacteria that bound to HeLa cells generated actin pedestals, less than 5% of cell-associated EHECΔCP_U harboring a vector control generated F-actin structures resembling pedestals (Figure 1A). These residual sites of actin assembly generally stained less intensely than wild-type pedestals (data not shown). In contrast, the $espF_U$-containing plasmid completely restored the pedestal-forming ability of EHECΔCP_U to wild-type levels (Figure 1A). Thus, the only gene located within CP_U that appears to be required for EHEC pedestal formation is the *espF*-homolog, $espF_U$.

The EspF protein encoded by the EPEC LEE is a proline-rich effector that disrupts intestinal barrier function and induces cell death, but does not contribute to actin pedestal formation (Crane et al., 2001; McNamara et al., 2001). However, a role in pedestal formation has not been explored for EspF encoded by the EHEC LEE. Moreover, in addition to *espF* and $espF_U$, EHEC possesses an ORF within another cryptic prophage, CP-933M, that potentially encodes a third proline-rich EspF-like protein, $EspF_M$ (Perna et al., 2001). This hypothetical protein is virtually identical to the proline-rich C-terminal 250 amino acids of $EspF_U$, but lacks a canonical initiation codon and an N-terminal sequence found in $EspF_U$ that is likely required for type III secretion. To determine which of the EspF-like genes are involved in pedestal formation, EHEC strains containing specific deletions in *espF*, $espF_M$, or $espF_U$ were generated and examined for the ability to trigger localized actin assembly. While deletions of *espF* and $espF_M$ did not affect pedestal formation by EHEC, the loss of $espF_U$ resulted in a dramatic reduction in the efficiency of pedestal formation, and in the intensity of the residual pedestals that were formed, similar to a strain lacking CP_U (Figure 1B). Hence, $espF_U$ is unique among the *espF*-like genes in its ability to contribute to actin assembly.

$EspF_U$ Localizes to Sites of Actin Nucleation following Translocation by the LEE-Encoded Type III Secretion System

To test whether $espF_U$ encodes a protein substrate for the LEE-encoded type III apparatus, pEspF$_U$-myc, a low copy number plasmid that expresses a derivative of $EspF_U$ fused at its C terminus to five copies of the c-*myc* epitope, was constructed. This plasmid was introduced into wild-type EHEC and EHECΔETTA1, a strain that lacks a functional LEE secretion pathway (Table 1). Since EHEC effectors that are transported by ETTA1 can be detected in liquid media (DeVinney et al., 1999), cultures of these two EHEC strains were separated into a pelleted

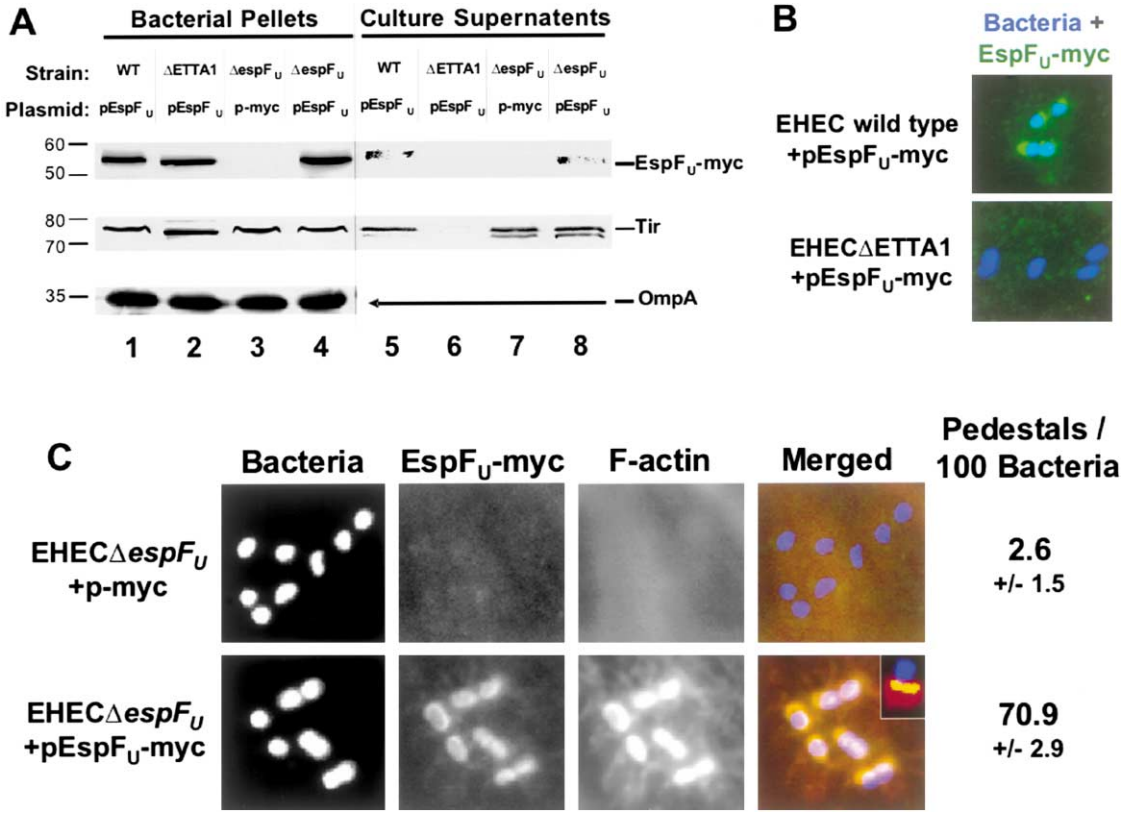

Figure 2. $EspF_U$ Localizes to Sites of Actin Nucleation following Translocation by the LEE-Encoded Type III Secretion System

(A) Wild-type EHEC, an EHEC strain lacking ETTA1, and an EHEC strain lacking $EspF_U$ were transformed with a control plasmid or a plasmid encoding myc-tagged $EspF_U$. Cultured strains were separated into bacterial and supernatant fractions prior to SDS-PAGE and immunoblotting for Tir and $EspF_U$-myc. Blotting for bacterial outer membrane protein A (OmpA) demonstrated similar protein quantities within pellet fractions (lanes 1–4). The amounts of bacteria loaded in lanes 1–4 are equal to 0.3 ml cultures; supernatent samples in lanes 5–8 are equivalent to 1.2 ml cultures. Positions of molecular weight standards (kDa) are shown to the left.

(B) HeLa cells infected with translocation-proficient and translocation-deficient EHEC strains harboring $pEspF_U$-myc were treated with DAPI to identify bacteria (blue) and with an anti-myc antibody to visualize $EspF_U$ (green). Anti-myc staining beneath bacteria was not observed if the cell monolayer was not permeabilized prior to addition of the antibody (not shown).

(C) HeLa cells infected with EHEC$\Delta espF_U$ derivatives were treated with DAPI to identify bacteria, with an anti-myc antibody to visualize $EspF_U$, and with phalloidin to stain F-actin. The magnified inset shows $EspF_U$-myc (yellow) localized at the tip of an actin pedestal (red) formed beneath a bacterium (blue). Pedestal formation efficiencies were quantitated as described in Figure 1.

bacterial fraction and a supernatant fraction and examined in immunoblots for the presence of myc-tagged $EspF_U$. Treatment of blotted bacterial samples with an anti-myc antibody indicated that $EspF_U$-myc was expressed equivalently in both strains as a 52 kDa protein (Figure 2A, lanes 1 and 2), a size consistent with the expected combined molecular weights of $EspF_U$ (42 kDa) and the myc-tag (10 kDa). However, as predicted for a substrate of ETTA1, $EspF_U$-myc was only detectable in the culture supernatant of the wild-type strain (Figure 2A, lanes 5 and 6).

To test whether the LEE secretory pathway also promoted entry of $EspF_U$-myc into mammalian cells, HeLa cells were infected with these same EHEC strains and examined microscopically. While $EspF_U$-myc was clearly visible within host cells beneath translocation-proficient EHEC, it was not detected in cells harboring translocation-deficient EHEC (Figure 2B), indicating that $EspF_U$ is indeed translocated and requires the LEE-encoded type III machinery in order to enter host cells.

These studies of the expression, secretion, and translocation of myc-tagged $EspF_U$ were performed in strain backgrounds in which the untagged version of this protein was presumably also present. To examine the same properties of epitope-tagged $EspF_U$ in the absence of endogenous $EspF_U$, $pEspF_U$-myc or a p-myc control was introduced into EHEC$\Delta espF_U$. As expected, the strain harboring $pEspF_U$-myc expressed, secreted, and translocated myc-tagged $EspF_U$ (Figure 2A, lanes 4 and 8; Figure 2C). $EspF_U$-myc also completely restored actin pedestal-forming ability to this strain (Figure 2C), indicating that the epitope-tagged derivative is functional. Consistent with a role for $EspF_U$ as an effector of pedestal formation, costaining for $EspF_U$-myc and F-actin demonstrated that $EspF_U$ primarily localized to tips of actin pedestals (Figure 2C, inset).

$EspF_U$ Does Not Modulate the Expression, Modification, or Membrane Localization of Tir

Tir, the only effector previously shown to be directly required for EHEC pedestal formation, is also known to localize within host cells at the tips of pedestals (DeVinney et al., 1999). One possible explanation for the inability of EHEC$\Delta espF_U$ to effectively form pedestals is that

Tir is not efficiently chaperoned through the type III secretory apparatus without $EspF_U$. However, examination of fractionated EHEC cultures demonstrated that the expression and secretion of Tir were equivalent in the presence or absence of $EspF_U$ (Figure 2A, lanes 3 and 4 and lanes 7 and 8).

After entry into the host cell, EHEC Tir is phosphorylated on serine and/or threonine residues, which increases its apparent molecular weight from 72 kDa to nearly 90 kDa (DeVinney et al., 1999). It has been suggested that EHEC encodes factors that facilitate these modifications of Tir to promote pedestal formation (Kenny, 2001). Therefore, to test whether $EspF_U$ affects Tir translocation or its subsequent modification, HeLa cells were infected with wild-type EHEC or with EHECΔ*espF$_U$*. Following removal of nonassociated bacteria, cells were lysed and immunoblotted for Tir. Consistent with the relationship of Tir translocation to its change in mobility, infection of cells with wild-type EHEC resulted in a shift in Tir migration from 72 kDa to nearly 90 kDa (Figure 3A, lanes 1 and 4). EHECΔ*espF$_U$* similarly delivered Tir into HeLa cells, and levels of translocation and modification were unaltered by the addition of $EspF_U$-myc (Figure 3A, lanes 5 and 6).

Upon insertion into the plasma membrane with its central domain exposed at the cell surface, Tir is maintained beneath sites of EHEC attachment because its ligand, the bacterial outer membrane protein intimin, binds to this region of Tir (DeVinney et al., 1999). Tir translocated in the absence of $EspF_U$ also displayed this localization pattern, as its N-terminal cytoplasmic domain was detectable in HeLa cells beneath EHECΔ*espF$_U$* in a manner indistinguishable from wild-type EHEC (Figure 3B). Hence, $EspF_U$ does not appear to influence the delivery, modification, or membrane localization of Tir.

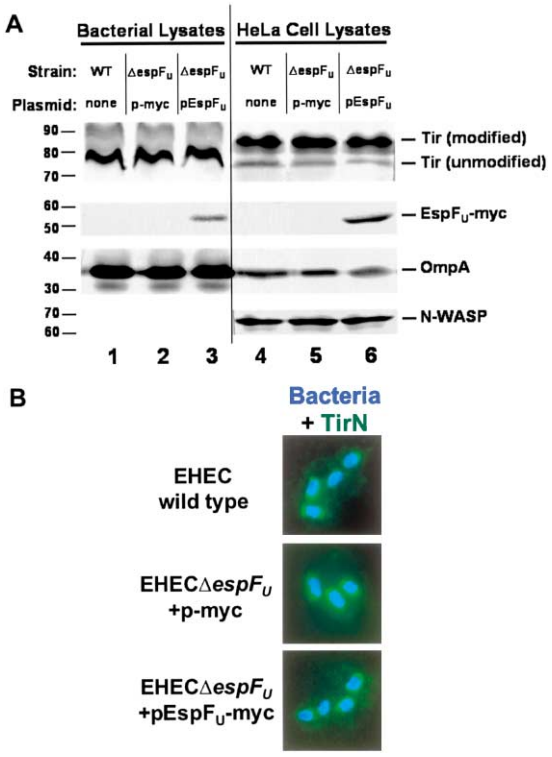

Figure 3. $EspF_U$ Does Not Regulate the Translocation, Modification, or Membrane Localization of Tir

(A) EHEC lysates (lanes 1–3) or lysates of EHEC-infected HeLa cells (lanes 4–6) were immunoblotted for Tir and $EspF_U$-myc. The position of the modified translocated form of Tir and the unmodified immature species of Tir are shown. OmpA immunoblotting demonstrated equivalent protein content within EHEC lysates (lanes 1–3) and similar levels of bacterial association with HeLa cells for each strain (lanes 4–6). N-WASP immunoblotting indicated similar protein quantities were present in HeLa lysates (lanes 4–6). The amounts of bacteria in lanes 1–3 are equal to 0.1 ml cultures; HeLa samples in lanes 4–6 are equivalent to 3 cm^2 of infected monolayers.

(B) HeLa cells infected with wild-type EHEC or with EHECΔ*espF$_U$* derivatives were treated with DAPI to identify bacteria (blue) and with antibodies to visualize the N-terminal cytoplasmic domain of Tir (TirN; green). TirN staining was not detected beneath control strains EHECΔ*tir* or EHECΔETTA1 (not shown).

$EspF_U$ Allows KC12, an EPEC Strain that Expresses EHEC Tir, to Efficiently Generate Actin Pedestals Independent of Nck Adaptors

The ability of EHECΔ*espF$_U$* to translocate Tir but not initiate actin assembly is strikingly similar to the phenotypes of EPEC strains engineered to express EHEC Tir (Campellone et al., 2002; DeVinney et al., 2001; Kenny, 2001). One such strain, KC12, is an EPEC derivative in which the endogenous chromosomal copy of *tir* has been replaced with sequence encoding an N-terminally HA-tagged version of EHEC Tir (Campellone et al., 2002). Tir translocated by KC12 localizes beneath adherent bacteria, but fails to efficiently trigger pedestal formation, presumably because EPEC lacks one or more effectors, exclusively present in EHEC, that promote actin assembly independent of tyrosine phosphorylation (Campellone et al., 2002; DeVinney et al., 2001; Kenny, 2001). A search of the EPEC genome database indicated that an *espF$_U$*-like gene was not present (our unpublished data). Therefore, to determine if $EspF_U$ is the only EHEC effector of pedestal formation missing from EPEC, p-myc and p$EspF_U$-myc were introduced into KC12. Similar to EHEC strains lacking $EspF_U$ (Figure 1), KC12 harboring the vector control formed pedestals only at low levels (Figure 4A). In contrast, the expression of $EspF_U$-myc by KC12 resulted in its translocation into host cells, and remarkably promoted the formation of pedestals at an efficiency equivalent to that of an EPEC strain expressing EPEC Tir (Figure 4A). Thus, $EspF_U$ is the only EHEC-specific effector necessary for localized actin assembly.

While EPEC utilizes its tyrosine phosphorylated Tir molecule to recruit Nck adaptor proteins and initiate actin polymerization, EHEC generates pedestals independently of Nck (Campellone et al., 2002; Gruenheid et al., 2001). Indeed, the inability of EHEC Tir to recruit Nck (Figure 4B) is likely responsible for its inability to function for actin assembly when expressed in KC12. To determine if Nck localized to pedestals formed by KC12 expressing $EspF_U$-myc, infected HeLa cells were examined microscopically. In contrast to wild-type EPEC, but like wild-type EHEC, KC12 + p$EspF_U$-myc did not recruit Nck (Figure 4B).

Since KC12 expressing $EspF_U$ generates pedestals without detectable Nck recruitment, $EspF_U$ may function to circumvent Nck-dependent pathways to actin assembly. To test this, Nck-proficient and Nck-deficient mouse embryonic fibroblasts (MEFs) (Bladt et al., 2003) were

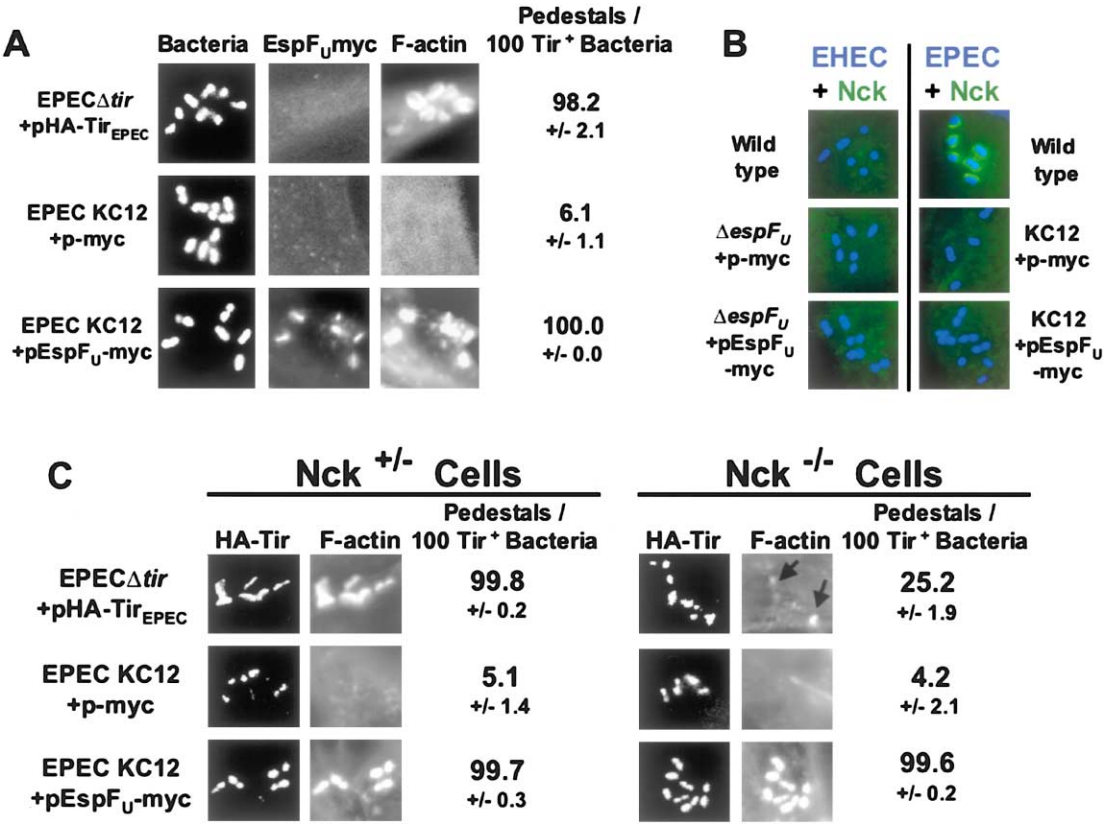

Figure 4. EspF$_U$ Allows KC12, an EPEC Strain that Expresses EHEC Tir, to Efficiently Generate Actin Pedestals Independent of Nck Adaptors

(A) HeLa cells were infected either with an EPEC strain that expresses HA-tagged EPEC Tir (top panels) or with derivatives of KC12, an EPEC strain that expresses HA-tagged EHEC Tir (middle and lower panels). Infected cells were treated with DAPI to identify bacteria, with an anti-myc antibody to visualize EspF$_U$, and with phalloidin to stain F-actin. Anti-myc staining was not detected beneath an EspF$_U$-expressing EPEC strain incapable of type III secretion (not shown). To measure pedestal formation efficiencies, bacteria that translocated Tir, as determined by HA-staining proximal to sites of attachment, were examined. The percentage of these Tir$^+$ bacteria associated with F-actin staining was quantitated. These criteria differ from those used to assess pedestal formation of bacteria expressing untagged Tir (e.g., Figures 1 and 2). Data are the means ($\pm$SD) of three separate experiments.

(B) HeLa cells infected with EHEC strains (left panels) or EPEC strains (right panels) were treated with DAPI to identify bacteria (blue) and with antibodies to visualize Nck (green).

(C) Nck-proficient cells (left panels) and Nck-deficient cells (right panels) infected with EPEC strains were treated with an anti-HA antibody to visualize translocated Tir and with phalloidin to stain F-actin. Arrows indicate sites of actin assembly in Nck$^{-/-}$ cells. Pedestal formation efficiencies were measured as described in (A). Pedestals generated by EPECΔ*tir* + pHA-Tir$_{EPEC}$ were similar in number and morphology to pedestals formed by wild-type EPEC (not shown).

infected with an EPEC strain that expresses its own tyrosine-phosphorylated Tir, or with KC12 expressing EspF$_U$. As previously observed (Gruenheid et al., 2001), the intensity and frequency of actin pedestal formations initiated by EPEC Tir were significantly reduced in cells lacking Nck (Figure 4C). In contrast, the KC12 derivative expressing EspF$_U$ generated pedestals at equivalent levels on both cell lines, and at efficiencies indistinguishable from pedestals formed by wild-type EPEC on Nck-proficient cells (Figure 4C). Hence, EspF$_U$ promotes localized actin assembly completely independent of Nck adaptor proteins.

EspF$_U$ Is Required for Efficient Recruitment of the N-WASP-Arp2/3 Actin Assembly Machinery

Tir is the only EHEC effector known to be required for recruitment of the N-WASP-Arp2/3 actin nucleating complex to sites of adherence (Goosney et al., 2001). To examine whether EspF$_U$ is also required for localization of these components, cells infected with EspF$_U$-deficient and EspF$_U$-proficient strains of EHEC and KC12 were stained for N-WASP and Arp3. Both N-WASP and Arp3 efficiently localized beneath EHEC and KC12 in an EspF$_U$-dependent manner (Figure 5A). Since delivery of EHEC Tir into the plasma membrane by either EHECΔ*espF$_U$* or KC12 is not sufficient to localize N-WASP or Arp2/3 (Figure 5A), EHEC Tir must somehow cooperate with EspF$_U$ in order to effectively recruit and subsequently activate these fundamental components of the actin assembly machinery.

Notably, EPEC KC12 and EHECΔ*espF$_U$* behave identically in all aspects of actin pedestal formation that have been tested, suggesting that these two strains are functionally equivalent. By analogy, expression of EspF$_U$ in KC12 apparently creates a strain that corresponds to wild-type EHEC in its method of pedestal formation.

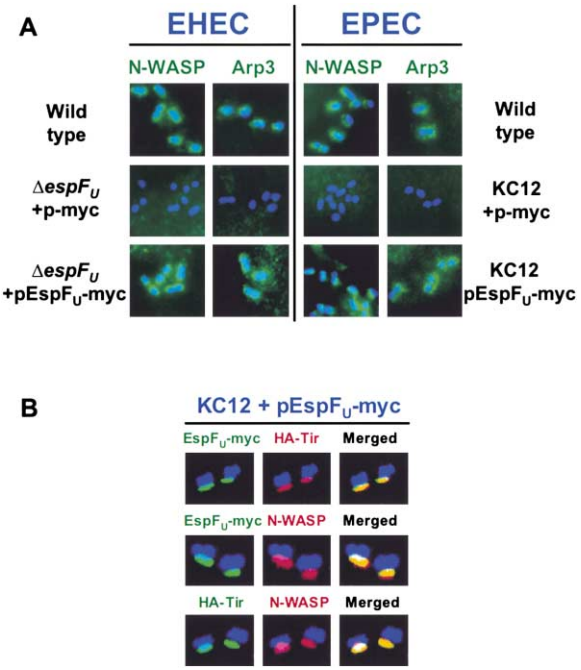

Figure 5. $EspF_U$ Is Required for Efficient Recruitment of N-WASP and the Arp2/3 Complex

(A) HeLa cells infected with the indicated EHEC strains (left panels) or EPEC strains (right panels) were treated with DAPI to identify bacteria (blue) and with antibodies to visualize N-WASP or Arp3 (each shown in green).

(B) HeLa cells infected with KC12 expressing $EspF_U$-myc were treated with DAPI to identify bacteria (blue) and with antibodies to visualize HA-tagged Tir, myc-tagged $EspF_U$, or endogenous N-WASP (each shown in either green or red). Pairwise colocalizations of these proteins appear yellow in the merged images.

Since EPEC strains bind to cultured cells and translocate effectors with a dramatically greater efficiency than EHEC strains, KC12 and its derivatives provide an optimal experimental system to study mechanisms of pedestal formation by EHEC.

$EspF_U$ Acts as an Intermediate between Tir and N-WASP during Actin Pedestal Formation

To investigate the relationship of Tir and $EspF_U$ during the formation of actin pedestals, a direct comparison of their localization was performed. Fluorescent antibody staining of HeLa cells infected with KC12 expressing $EspF_U$ demonstrated that HA-tagged EHEC Tir and myc-tagged $EspF_U$ precisely colocalized beneath adherent bacteria (Figure 5B), suggesting that they may physically associate during pedestal formation. To test whether Tir and $EspF_U$ interact within mammalian cells, infected HeLa cells were lysed, and after removal of bacteria, EHEC Tir was immunoprecipitated using an antibody to its HA-epitope. Western blotting demonstrated that both the modified and unmodified forms of Tir were similarly precipitated in the presence or absence of $EspF_U$ (Figure 6A, lanes 5 and 6). Interestingly, blotting of these same samples with an anti-myc antibody indicated that $EspF_U$ coprecipitated with Tir (Figure 6A, lane 6). This interaction was specific, because neither Tir nor $EspF_U$ was precipitated from HeLa lysates when a control antibody was used (Figure 6A, lanes 3 and 4) or when anti-HA precipitations were performed on lysates containing an untagged version of EHEC Tir (data not shown).

Since $EspF_U$ associates with Tir at the tip of the pedestal, the site where actin polymerization occurs, its role as an effector during pedestal formation may be to mediate an interaction between Tir and actin assembly components. Indeed, both Tir and $EspF_U$ precisely colocalized in HeLa cells with N-WASP (Figure 5B). To test whether $EspF_U$ is capable of interacting with N-WASP, cells infected with KC12 derivatives were lysed and supplemented with recombinant N-WASP prior to immunoprecipitation of myc-tagged $EspF_U$. Western blotting demonstrated that N-WASP coprecipitated with $EspF_U$-myc (Figure 6B, lane 7). In contrast, N-WASP was not precipitated by an anti-myc antibody in the absence of $EspF_U$ (Figure 6B, lane 6) or by a control antibody in the presence of $EspF_U$ (Figure 6B, lane 5), indicating that the interaction of $EspF_U$ with N-WASP is specific.

The C Terminus of $EspF_U$ Binds to the GBD of N-WASP

The N termini of many *E. coli* effectors function to promote translocation into the mammalian cell, suggesting that the ability of $EspF_U$ to interact with N-WASP might lie within its C-terminal proline-rich region. Therefore, the 79-residue N terminus of $EspF_U$, a segment homologous to the translocation signal found within EspF (McNamara et al., 2001), was replaced with a 6-His tag. To determine if $EspF_U$ can bind directly to Tir or N-WASP, this His-tagged derivative of $EspF_U$ was subjected to SDS-PAGE, transferred to immobilon membranes, and probed with purified recombinant N-WASP or Tir. Bound N-WASP or Tir was then detected with the appropriate specific antibodies. Conversely, recombinant N-WASP transferred to immobilon membranes was probed with soluble purified $EspF_U$ or Tir. These Far Western assays revealed no interactions between Tir and $EspF_U$ or Tir and N-WASP. However, they clearly demonstrated that N-WASP bound to immobilized $EspF_U$ and not to unrelated proteins (Figure 6C, top) and, similarly, that His-tagged $EspF_U$ bound to immobilized N-WASP (Figure 6C, bottom). Hence, the C terminus of $EspF_U$ is capable of binding to N-WASP directly, and in the absence of any other mammalian or EHEC factors.

To further explore the ability of $EspF_U$ to bind N-WASP, derivatives of these two proteins were examined in a yeast two-hybrid interaction system. $EspF_U$ fragments were fused to the Gal4 transcriptional activation domain, while N-WASP derivatives were fused to the LexA DNA binding domain. Pairwise combinations of these $EspF_U$- and N-WASP-fusion proteins were expressed in yeast strain L40, which harbors *lacZ* and *HIS3* reporter genes. To evaluate the relative strength of the interaction between $EspF_U$ and N-WASP, expression of the *lacZ* reporter was determined in liquid β-galactosidase assays, while *HIS3* reporter activity was assessed by plating cultures on media lacking histidine but containing increasing concentrations of 3-aminotriazole (3-AT), a competitive inhibitor of His3p. All interactions were measured relative to the expression of single LexA-N-WASP derivatives in the presence of the corresponding (non-fused) Gal4 vector controls. Consistent with Far Western

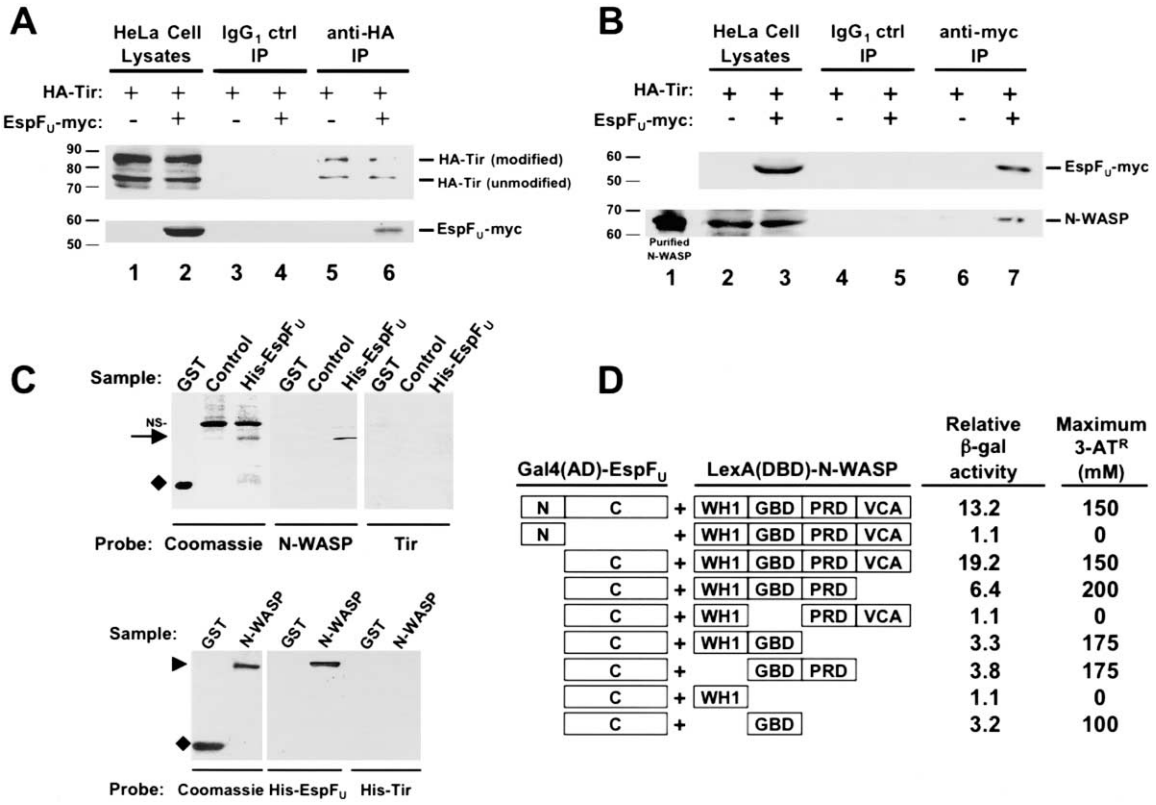

Figure 6. $EspF_U$ Associates with Tir and Binds the GBD of N-WASP

(A) HeLa cells were infected with KC12 harboring p-myc or p$EspF_U$-myc and lysed. These samples were then left untreated (lanes 1 and 2) or were subjected to immunoprecipitation with a control antibody (lanes 3 and 4) or an anti-HA antibody (lanes 5 and 6). Cell lysates and immunoprecipitates were then blotted for HA-tagged Tir and myc-tagged $EspF_U$. Samples in lanes 1 and 2 equal 1.5 cm^2 of infected monolayers and are equivalent to approximately 1/12 of the amount of lysate in IP-associated lanes.

(B) HeLa cells infected and lysed as described in (A) were either left untreated (lanes 2 and 3) or were supplemented with recombinant N-WASP prior to immunoprecipitation with a control antibody (lanes 4 and 5) or an anti-myc antibody (lanes 6 and 7). Lane 1 shows 1/10 of the amount of N-WASP used to supplement HeLa lysates. Samples in lanes 2 and 3 equal 5 cm^2 of infected HeLa cell monolayers and are equivalent to approximately 1/3 of the amount of lysate in IP-associated lanes.

(C) Purified proteins from *E. coli* either expressing GST, harboring a His-tagged vector control, or expressing His-$EspF_U$ (top panel) were separated by SDS-PAGE, transferred to PVDF membranes, and probed with recombinant N-WASP or EHEC Tir. Bound proteins were detected with N-WASP or Tir antibodies. Coomassie blue staining shows the relative protein content within each sample. Migratory positions of GST (diamond), His-$EspF_U$ (arrow), and a nonspecific (NS) *E. coli* protein are indicated. The N-WASP antibody does not crossreact with $EspF_U$ (not shown). Purified GST and N-WASP were similarly treated (bottom panels), and probed with His-$EspF_U$ or His-Tir. Bound protein was detected with an anti-His antibody. The migratory-position of N-WASP (arrowhead) is indicated.

(D) Gal4-fusions to fragments of $EspF_U$ and LexA-fusions to derivatives of N-WASP are depicted. Fusion proteins were coexpressed in a yeast strain that possesses LexA binding sites within the *lacZ* and *HIS3* promoters. Reporter activation was measured by quantitating β-galactosidase activity (fold increase) and 3-AT resistance (mM increase) relative to control yeast strains that expressed single or LexA-fusions. Data are the means of triplicate samples; similar patterns of reporter activation were observed in two to four independent experiments.

analyses, a fragment of $EspF_U$ containing only its C-terminal proline-rich region was sufficient to interact with full-length N-WASP, as determined by strong activation of both the *lacZ* and *HIS3* reporters (Figure 6D). In contrast, the N-terminal putative translocation-domain of $EspF_U$ did not associate with N-WASP (Figure 6D).

N-WASP binds and activates the Arp2/3 complex with its C-terminal verprolin-cofilin-acidic (VCA) region; sequences upstream of this fragment can control the activity and/or localization of N-WASP (reviewed in Higgs and Pollard, 2001; Welch and Mullins, 2002). These regulatory domains can be functionally divided into a WASP-homology-1 (WH1) region that interacts with WIP-family proteins, a GTPase binding domain (GBD) that binds to activated Cdc42, and a proline-rich domain (PRD) that interacts with SH3-containing adaptor proteins like Nck and Grb2 (Figure 6D; Higgs and Pollard, 2001). Interestingly, a portion of the GBD was recently revealed to be critical for recruitment to sites of EHEC adherence (Lommel et al., 2004). To define the region of N-WASP that harbors its $EspF_U$ binding activity, a series of N-WASP derivatives containing deletions in one or more of these domains were tested for the ability to interact with $EspF_U$. These deletion analyses demonstrated that only those N-WASP constructs possessing an intact GBD were capable of interacting with $EspF_U$ (Figure 6D). In fact, an N-WASP fragment containing the GBD alone was sufficient to promote this interaction (Figure 6D).

Hence, by binding the GBD of N-WASP, $EspF_U$ is apparently capable of directly recruiting the actin assembly machinery to sites of EHEC adherence.

Discussion

Much of what is known about how attaching and effacing pathogens stimulate actin pedestal formation has been uncovered by studies utilizing EPEC. These analyses demonstrate that clustering of tyrosine phosphorylated Tir in the plasma membrane is necessary and sufficient to trigger localized actin assembly. EHEC, a pathogen closely related to EPEC, also generates pedestals in a Tir-dependent manner, but without detectable phosphotyrosines. In fact, when expressed in an EPEC strain background, EHEC Tir does not efficiently promote actin assembly, suggesting that EHEC requires additional molecules in order to stimulate pedestal formation. We hypothesized that such effectors would be encoded by an EHEC pathogenicity island distinct from the LEE, and utilizing a RAPID screening technique now reveal that $EspF_U$ is a second translocated EHEC effector critical for actin pedestal formation.

The essential role that tyrosine kinase signaling plays during pedestal formation by EPEC is primarily due to the fact that phosphorylation of Tir residue Y474 generates a binding site for mammalian Nck adaptors (Campellone et al., 2002; Gruenheid et al., 2001). In this study, we confirm previous work demonstrating that Nck is required for efficient pedestal formation by EPEC (Gruenheid et al., 2001). However, while EPEC was not previously reported to form any pedestals on Nck-deficient cells, we found that the absence of Nck was associated with only a 4-fold decrease in the efficiency of localized actin assembly. These F-actin structures colocalize with sites of translocated Tir, and although they sometimes stain less intensely for F-actin, they appear morphologically similar to pedestals formed on Nck-proficient cells (Figure 4C; data not shown). Quantitation was not provided in the earlier study, and differences in the methods used to assess pedestal formation may contribute to these partially discrepant results. Since a mutation of Y474 in the Nck binding site of Tir abolishes EPEC pedestal formation (Kenny, 1999), we hypothesize that this Nck-independent EPEC signaling pathway requires Y474 and could be mediated by another SH2-domain-containing protein.

While EPEC requires Nck for maximal efficiency of pedestal formation, EHEC forms pedestals without detectable Nck recruitment (Campellone et al., 2002) and with full efficiency on cells that do not contain Nck (Gruenheid et al., 2001). Remarkably, the introduction of $EspF_U$ into KC12, an EPEC derivative that expresses EHEC Tir, is sufficient to convert this strain into one that generates pedestals at nearly every site of Tir translocation on Nck-deficient cells, demonstrating that $EspF_U$ is the EHEC effector that allows efficient bypass of Nck signaling pathways. Hence, Tir and $EspF_U$ are likely to be the only translocated molecules involved in pedestal formation by EHEC.

$EspF_U$ does not display any obvious sequence homology to known regulators of actin assembly, but is 25% identical (35% similar) to EspF, an effector encoded by the EHEC and EPEC LEE elements. Notably, much of the homology between EHEC EspF and $EspF_U$ extends over the first 60–70 residues of the two proteins, which are 40% identical (65% similar). Since this N terminus of EspF promotes type III translocation (McNamara et al., 2001), it seems likely that the corresponding region of $EspF_U$ also provides this capability. Indeed, one explanation for the inability of $EspF_M$ to contribute to pedestal formation (Figure 1B) is that it cannot enter host cells because it lacks this domain.

One critical function of translocated EspF is to promote a disruption of tight junctions and increase the permeability of epithelial monolayers (McNamara et al., 2001). Interestingly, $EspF_U$ also possesses this activity (Viswanathan et al., 2004), indicating the existence of some functional overlap between these two effectors. However, $EspF_U$ is unique in its ability to stimulate localized actin assembly, because an EHEC *espF* mutant forms pedestals at normal levels (Figure 1), and the introduction of EHEC *espF* into KC12 does not increase pedestal formation (our unpublished data).

Since the C termini of EspF and $EspF_U$ are quite divergent, with most similarity due to the fact that they are both rich in proline residues, we postulate that this region of $EspF_U$ contains its actin signaling activity. Consistent with this hypothesis, Far Western and yeast two-hybrid analyses demonstrate that the C terminus of $EspF_U$ is necessary and sufficient to promote an interaction with N-WASP. Within this domain, $EspF_U$ harbors 6 nearly identical 47-residue repeats consisting of 21% proline, including 22 putative SH3-domain binding (PxxP) motifs.

In spite of the fact that N-WASP does not possess any SH3 domains, two-hybrid assays indicate that the $EspF_U$ C terminus is capable of interacting with its GTPase binding domain. Interestingly, a region within the GBD was recently determined to be sufficient to promote N-WASP localization to sites of EHEC adherence (Lommel et al., 2004). These results, taken together with the observation that Rho-family GTPases do not appear to be critical for actin assembly during EHEC infections (Campellone and Leong, 2003), therefore suggest that $EspF_U$ directly recruits N-WASP to sites of bacterial attachment by binding the GBD.

$EspF_U$ may merely serve to localize N-WASP, or it could also promote N-WASP activation. Notably, the region within the GBD that is required for EHEC recruitment lies downstream of the minimal Cdc42-Rac-interactive binding (CRIB) motif (Lommel et al., 2004). Since CRIB binding by Cdc42 activates N-WASP by altering its autoinhibited conformation (reviewed in Higgs and Pollard, 2001), $EspF_U$ binding to this adjacent region may similarly result in N-WASP activation. The surface protein IcsA/VirG of the intracellular pathogen *Shigella flexneri* can also stimulate localized actin assembly by recruiting GBD-containing derivatives of N-WASP (reviewed in Goldberg, 2001). While IcsA and $EspF_U$ do not display any sequence homology, it is tempting to speculate that they can each recognize the GBD in a manner that enhances the ability of N-WASP to stimulate the Arp2/3 complex.

In addition to binding N-WASP, the mechanism by

which $EspF_U$ promotes actin pedestal formation likely involves its ability to associate with Tir, since the two molecules coprecipitate from mammalian cell lysates. The region of EHEC Tir responsible for signaling is not defined, but the observation that EHEC strains can utilize EPEC Tir to form pedestals even when a Nck-mediated pathway is abolished by a Y474F mutation (Campellone et al., 2002; DeVinney et al., 2001) suggests that the critical cytoplasmic region within EHEC Tir is also conserved in EPEC Tir. In the simplest model, $EspF_U$ directly binds this portion of Tir to promote N-WASP recruitment to sites of bacterial attachment. However, recombinant Tir does not appear to bind to $EspF_U$ in Far Western (Figure 6) or yeast two-hybrid assays (our unpublished data), suggesting that the interaction between Tir and $EspF_U$ is indirect. Since Tir and $EspF_U$ are likely the only two bacterial proteins directly involved in EHEC-mediated pedestal formation, additional molecules required for their association are presumably of mammalian origin.

Consistent with previous work (DeVinney et al., 1999), we observed that an EHEC strain lacking Tir is completely incapable of generating actin pedestals (Figure 1). In contrast, while strains lacking $EspF_U$ are severely defective at triggering localized actin assembly, they can still form pedestal-like structures at approximately 5% of wild-type levels in the presence of EHEC Tir. These results suggest that EHEC Tir can inefficiently stimulate actin assembly by itself, whereas $EspF_U$ promotes actin polymerization only in the presence of Tir. $EspF_U$ may function as a potent enhancer of an ordinarily weak signaling ability of Tir, perhaps by stabilizing its interaction with one or more host molecules that otherwise bind with low efficiency. This host protein does not appear to be N-WASP, because an interaction between Tir and N-WASP has not been detected in co-IP or Far Western assays (Figure 6; our unpublished data). Given the presence of proline-rich sequences in its C terminus, we hypothesize that $EspF_U$ interacts with at least one host protein that contains an SH3 domain and may also bind to Tir.

Much of what is known about how cells regulate actin assembly via N-WASP and the Arp2/3 complex has come from studies of intracellular bacteria, like *Listeria* and *Shigella*, which form F-actin comet tails in the cytoplasm of infected cells. More recently, pathogens that stimulate actin polymerization at the cell surface have revealed new insights into transmembrane signaling pathways that activate these molecules. Two such microbes, vaccinia virus and EPEC, activate tyrosine kinase signaling cascades and recruit Nck adaptors to stimulate localized actin assembly. In contrast, EHEC has acquired the ability to initiate transmembrane signaling independently of phosphotyrosines and Nck by translocating $EspF_U$ in addition to Tir. While $EspF_U$ interacts with Tir and recruits N-WASP to sites of EHEC adherence, the nature and significance of these associations during pedestal formation have not been determined. Defining the critical signaling activities of EHEC Tir and $EspF_U$ and identifying the additional mammalian components that they interact with is certain to provide new insights into cellular control of actin assembly and the manner in which pedestal formation contributes to EHEC virulence.

Experimental Procedures

Strains, Cell Lines, and Plasmids

All EHEC strains used in this study were derived from TUV93-0, a Shiga-toxin-deficient form of EDL933 (Campellone et al., 2002). Gene replacements were performed by electroporating PCR-generated recombination substrates containing the *cat* gene flanked by 50 nucleotides of island-targeting sequences into TUV93-0 harboring λ-Red plasmid pKM201 as described previously (Murphy and Campellone, 2003). Proper replacement of EHEC ORFs with *cat* was confirmed by generating specific PCR products using primers flanking the targeted region of the chromosome and by the absence of products using primers within the deleted region. EHECΔ*espF* (KC40) (Murphy and Campellone, 2003) contains a *cat* replacement of codons 18–232, EHECΔ$espF_M$ (KC42) contains a replacement encompassing the entire ORF, and EHECΔ$espF_U$ (KC44) contains a replacement of codons 18–368. EHECΔ*tir* (KC5), EHECΔETTA1 (KC30), and EPEC KC12 have been described (Campellone et al., 2002; Murphy and Campellone, 2003).

Bacterial and Mammalian Cell Culture

For routine passage, *E. coli* strains were cultured in LB at 37°C. EHEC mutants harboring the *cat* gene were grown in media containing 10–15 μg/ml chloramphenicol. None of these mutants appeared to have any obvious growth defects under these conditions. However, no recombinants were generated in three attempts to delete O-islands #28, #57, and #173–175. For maintenance of $EspF_U$ expression plasmids, media were supplemented with 20 μg/ml tetracycline or 35 μg/ml kanamycin (see below). Prior to infections, bacteria were cultured in DMEM+100 mM HEPES (pH 7.4) in 5% CO_2 to enhance type III secretion. HeLa cells, Nck1/Nck2-deficient MEFs, and Nck1-rescued MEFs (Bladt et al., 2003) were cultured in DMEM+10% FBS.

Complementation Plasmids

Vector pKC272 is the tet^R derivative of the medium copy number plasmid pTP809 (Murphy et al., 2000). To create p$EspF_U$ (pKC321; Figure 1), the sequence from 425 bp upstream through 125 bp downstream of the $espF_U$ ORF was PCR amplified from EDL933 genomic DNA using primers ATAAGAATGCGGCCGCAAGTATATCC CGATACATCATGCTCTC + ATAAGAATGCGGCCGCGCTTCACAA AACCGGAGTCCG and cloned into the NotI site of pKC272. To construct p-myc (pKC469), sequences 450 bp upstream and 530 bp downstream of $espF_U$ were amplified using primers CTCTCTTCTAG ATAAAGGAGCAAAAGTATA + ATAAGAATGCGGCCGCCATATGGA TTACCTTATAAGTAATTTTAGTTCTCC, and ATCATCCTGCAGTGAT TATAATATAATTACCTATATTAGCTCTG + ATCATCGAGCTCCTT GCCCCCAAAGATACCACA, respectively. A fragment encoding five copies of the c-*myc* epitope was amplified from pCS2+MT (a gift from S. Rankin, Harvard Medical School) with ATAAGAATGCGGCC GCGGATCCCATCGATTTAAAGCTATG + CTAGTCTAGACTGCAG TTAGGTGAGGTCGCCCAAGCTCTC. Following 4-way ligation, a fragment containing *myc* between EHEC flanking sequences was cloned into the XbaI and SacI sites of the low copy number kan^R vector pK187 (Campellone et al., 2002) to create p-myc. $EspF_U$ was amplified using CCGGAATTCCATATGATTAACAATGTTTCTTCACT TTTTCC + CGCGGATCCCGAGCGCTTAGATGTATTAATGCC and cloned into the NdeI and BamHI sites upstream of myc within p-myc to create p$EspF_U$-myc (pKC471; Figure 2 and subsequent figures).

Mammalian Cell Infections

For microscopic analyses of EHEC infections, HeLa cells grown to 50%–90% confluency on 12 mm glass coverslips were infected with 10^6 bacteria in DMEM+3% FBS+25 mM HEPES for 3.5 hr, washed with PBS, and incubated for a further 1.5 hr in fresh medium prior to fixation. EPEC infections of HeLa cells and MEFs were performed with 10^5 and 10^6 bacteria, respectively, for 3.5 hr. Greater numbers of EPEC were required for infection of MEFs due to inefficiencies of binding and effector translocation into these cell lines; EHEC strains interacted with MEFs at levels too low to allow strict quantitation of pedestal formation (our unpublished data). For biochemical analyses, HeLa cells grown in 9.5 cm^2 wells were infected with 3×10^7 EHEC for 3.5 hr, washed, and incubated for a further 1.5 hr. In

some experiments, non-intimately associated bacteria were killed with media containing 50 μg/ml gentamicin for 30 min. EPEC infections were performed with 10^7 bacteria for 3.5 hr.

Immunofluorescence Microscopy

Infected monolayers were fixed in PBS+2.5% paraformaldehyde for 20 min and permeabilized with 0.1% Triton-X-100 as described previously (Campellone et al., 2002). Cells were treated with either mouse anti-myc mAb 9E10 (diluted 1:250 in PBS+1%BSA; Sigma), rabbit anti-TirN (1:750; a gift from A. Donohue-Rolfe, Tufts Veterinary School), rabbit anti-Nck (1:150; Upstate), mouse anti-HA mAb HA.11 (1:500; Covance), rabbit anti-N-WASP (1:1000; a gift from S. Rankin), or rabbit anti-Arp3 (1:150; a gift from R. Isberg, Tufts University) prior to treatment with Alexa488-conjugated secondary antibodies (1:150; Molecular Probes). Bacteria were detected by treatment with 1 μg/ml DAPI, and F-actin was identified by staining with Alexa568-phalloidin (1:100; Molecular Probes). For colabeling of N-WASP with either Tir or $EspF_U$, cells were simultaneously treated with anti-N-WASP and either HA.11 or 9E10, followed by Alexa488-anti-mouse and Alexa568-anti-rabbit. For colabeling of $EspF_U$ and Tir, cells were successively treated with 9E10, Alexa488-anti-mouse, biotinylated HA.11 (1:250), and Alexa568-streptavidin. Pedestal formation efficiency was quantitated either by counting the percentage of cell-associated bacteria or the percentage of sites of translocated Tir that were associated with intense F-actin staining. 50 randomly chosen cells harboring isolated regions of 5–20 bacteria per cell were examined for each strain in three separate experiments. A minimum of 420 bacteria were counted per 50 cells.

Fractionation of EHEC Cultures

EHEC strains were grown with agitation in LB for 8 hr at 37°C prior to being diluted 500-fold into DMEM+100 mM HEPES. Following 14 hr growth without agitation in 5% CO_2, these cultures were diluted 1:20 into M9 salts+0.2% glucose+44 mM $NaHCO_3$ and incubated for an additional 5 hr. Bacteria were collected by centrifugation, washed twice with 20% glycerol, and resuspended in SDS-PAGE sample buffer. Culture supernatants were sterilized with 0.22 μm filters, supplemented with 1 mM PMSF, and 10 μg/ml each of pepstatin, leupeptin, and aprotinin (Sigma), and concentrated 50-fold using centrifugal filters (Amicon) prior to resuspension in sample buffer.

HeLa Cell Lysate Preparation and Immunoprecipitation

For analyses of total HeLa cell lysates, infected monolayers were collected in PBS+2 mM EDTA, washed with PBS, and lysed with lysis buffer (50 mM Tris HCl [pH 8.0], 150 mM NaCl, 1% Triton-X-100, PMSF, pepstatin, leupeptin, and aprotinin) prior to resuspension in sample buffer. For comparison to bacterial lysates, EHEC grown in DMEM+100 mM HEPES were collected by centrifugation, washed twice with 20% glycerol, and resuspended in sample buffer. For immunoprecipitations, infected HeLa cells were treated with lysis buffer and collected with a cell scraper. Cellular debris and bacteria were removed by centrifugation for 15 min at 10,000 g at 4°C. In some experiments, lysates were supplemented with purified recombinant N-WASP (a gift from S. Rankin) to enhance sensitivity. Lysates were mixed with either HA.11, 9E10, or an IgG_1 control antibody (anti-GFP; Clontech) at a ratio of 0.75 μg mAb/well lysate for 1.5 hr prior to precipitation with ProteinG magnetic microbeads (Miltenyi) for 45 min. After three washes with lysis buffer, precipitated proteins were collected from microbeads by boiling in sample buffer.

Immunoblotting

Protein samples mixed with loading buffer were boiled for 10 min. Debris was removed by centrifugation prior to 10% SDS-PAGE and transfer to PVDF membranes. Membranes were blocked with PBS+5% milk (PBSM) for 45 min before incubation with biotinylated 9E10 (diluted 1:300 in PBSM), rabbit anti-TirM (1:2000; Campellone et al., 2004), rabbit anti-OmpA (1:10000), anti-N-WASP (1:2000), or biotinylated HA.11 (1:500) for 2.5 hr. Membranes were washed, treated with anti-rabbit or anti-biotin secondary antibodies, and developed as described previously (Campellone et al., 2002). All experiments yielded similar results on at least three independent occasions.

Far Western Blots

Sequence encoding residues 80–384 of $EspF_U$ were PCR-cloned into the PstI and XbaI sites downstream of sequences encoding a 6-His tag and poly-glycine linker within the expression vector pEXP (Panomics) to create pKC508. After expression in *E. coli* strain BL21(DE3/pLysS), His-tagged $EspF_U$ was purified using a His-spin protein miniprep kit (Zymo Research). C-terminally His-tagged EHEC Tir was generously provided by Loranne Magoun. Purified GST, N-WASP, His-tagged $EspF_U$, or a sample from *E. coli* harboring pEXP were subjected to 10% SDS-PAGE, and transferred to PVDF membranes. Membranes were treated with N-WASP, His-tagged $EspF_U$, or His-tagged Tir (0.5 μg/ml each) and bound protein was detected with anti-N-WASP, anti-TirM, or anti-His (1:2500; Sigma) antibodies as described previously (Campellone, et al., 2002). Similar results were observed in multiple independent experiments.

Yeast Two-Hybrid Fusion Constructs

The two-hybrid expression vectors pGAD424 and pBTM116, as well as reporter strain L40, were previously utilized to define the interaction between EHEC Tir and intimin, and have been described in detail (Liu et al., 2002). DNA fragments encoding residues 1–384, 1–88, or 80–384 of $EspF_U$ were generated by PCR using various combinations of primers CCGGAATTCCATATGATTAACAATGTT TCTTCACTTTTTCC, CGCGGATCCCGAGCGCTTAGATGTATTAAT GCC, CGCGGATCCTATCAGGCGCTGCCTCACATTAGGA, and CCG GAATTCCTTCCTAATGTGAGGCAGCGCCTGATACAA, and cloned into the EcoRI and BamHI sites of pGAD424. DNA fragments encoding full-length rat N-WASP (WH1-GBD-PRD-VCA; residues 1–501), WH1-GBD-PRD (1–400), WH1-GBD (1–273), GBD-PRD (151–400), WH1 (1–150), and GBD (151–273) were similarly cloned into the EcoRI and PstI sites of pBTM116 after PCR-amplification from a pCS2+MT template. A DNA segment encoding residues 151–258 of full-length N-WASP was deleted by inverse PCR to create WH1-PRD-VCA.

Yeast Two-Hybrid Assays

Pairwise combinations of $EspF_U$- and N-WASP-fusion proteins were expressed in yeast strain L40. β-galactosidase reporter activity was determined in liquid ONPG assays of stationary-phase yeast cultures as described previously (Liu et al., 2002), while HIS3 reporter activity was assessed by spotting 5 μl of those yeast cultures on media containing 0, 25, 50, 75, 100, 125, 150, 175, or 200 mM 3-aminotriazole (3-AT) and scoring for large colony formation after 48 hr of growth. Several WH1-domain-containing constructs stimulated some activation of reporter genes in the absence of a Gal4-$EspF_U$ binding partner. Therefore, all interactions were measured relative to the highest level of autoactivation observed following expression of single LexA-N-WASP derivatives in the presence of their corresponding (nonfused) vector controls.

Acknowledgments

We thank Gail Hecht for communication of unpublished results, Tony Pawson for MEF cells, Art Donohue-Rolfe for Tir antiserum, Ralph Isberg for Arp3 antiserum, Susannah Rankin and Marc Kirschner for pCS2+MT, N-WASP antiserum, and recombinant N-WASP, Kenan Murphy for advice on Red-mediated recombineering, and Donald Tipper for comments on this manuscript. This work was supported by NIH-R01-AI46454 to J.M.L.

Received: April 20, 2004
Revised: May 28, 204
Accepted: May 28, 2004
Published: August 9, 2004

References

Bladt, F., Aippersbach, E., Gelkop, S., Strasser, G.A., Nash, P., Tafuri, A., Gertler, F.B., and Pawson, T. (2003). The murine Nck SH2/SH3 adaptors are important for the development of mesoderm-derived embryonic structures and for regulating the cellular actin network. Mol. Cell. Biol. *23*, 4586–4597.

Campellone, K.G., and Leong, J.M. (2003). Tails of two Tirs: actin

pedestal formation by enteropathogenic *E. coli* and enterohemorrhagic *E. coli* O157:H7. Curr. Opin. Microbiol. *6*, 82–90.

Campellone, K.G., Giese, A., Tipper, D.J., and Leong, J.M. (2002). A tyrosine-phosphorylated 12-amino-acid sequence of enteropathogenic *Escherichia coli* Tir binds the host adaptor protein Nck and is required for Nck localization to actin pedestals. Mol. Microbiol. *43*, 1227–1241.

Campellone, K.G., Rankin, S., Pawson, T., Kirschner, M.W., Tipper, D.J., and Leong, J.M. (2004). Clustering of Nck by a 12-residue Tir phosphopeptide is sufficient to trigger localized actin assembly. J. Cell Biol. *164*, 407–416.

Cantey, R.J., and Moseley, S.L. (1991). HeLa cell adherence, actin aggregation, and invasion by nonenteropathogenic *Escherichia coli* possessing the *eae* gene. Infect. Immun. *59*, 3924–3929.

Celli, J., Deng, W., and Finlay, B.B. (2000). Enteropathogenic *Escherichia coli* (EPEC) attachment to epithelial cells: exploiting the host cell cytoskeleton from the outside. Cell. Microbiol. *2*, 1–9.

Court, D.L., Sawitzke, J.A., and Thomason, L.C. (2002). Genetic engineering using homologous recombination. Annu. Rev. Genet. *36*, 361–388.

Crane, J.K., McNamara, B.P., and Donnenberg, M.S. (2001). Role of EspF in host cell death induced by enteropathogenic *Escherichia coli*. Cell. Microbiol. *3*, 197–211.

Deibel, C., Kramer, S., Chakraborty, T., and Ebel, F. (1998). EspE, a novel secreted protein of attaching and effacing bacteria, is directly translocated into infected host cells, where it appears as a tyrosine-phosphorylated 90 kDa protein. Mol. Microbiol. *28*, 463–474.

DeVinney, R., Stein, M., Reinscheid, D., Abe, A., Ruschkowski, S., and Finlay, B.B. (1999). Enterohemorrhagic *Escherichia coli* O157:H7 produces Tir, which is translocated to the host cell membrane but is not tyrosine phosphorylated. Infect. Immun. *67*, 2389–2398.

DeVinney, R., Puente, J.L., Gauthier, A., Goosney, D., and Finlay, B.B. (2001). Enterohaemorrhagic and enteropathogenic *Escherichia coli* use a different Tir-based mechanism for pedestal formation. Mol. Microbiol. *41*, 1445–1458.

Donnenberg, M.S., and Whittam, T.S. (2001). Pathogenesis and evolution of virulence in enteropathogenic and enterohemorrhagic *Escherichia coli*. J. Clin. Invest. *107*, 539–548.

Elliott, S.J., Yu, J., and Kaper, J.B. (1999). The cloned locus of enterocyte effacement from enterohemorrhagic *Escherichia coli* O157:H7 is unable to confer the attaching and effacing phenotype to *E. coli* K-12. Infect. Immun. *67*, 4260–4263.

Frankel, G., Phillips, A.D., Rosenshine, I., Dougan, G., Kaper, J.B., and Knutton, S. (1998). Enteropathogenic and enterohaemorrhagic *Escherichia coli*: more subversive elements. Mol. Microbiol. *30*, 911–921.

Goldberg, M.B. (2001). Actin-based motility of intracellular microbial pathogens. Microbiol. Mol. Biol. Rev. *65*, 595–626.

Goosney, D.L., DeVinney, R., and Finlay, B.B. (2001). Recruitment of cytoskeletal and signaling proteins to enteropathogenic and enterohemorrhagic *Escherichia coli* pedestals. Infect. Immun. *69*, 3315–3322.

Gruenheid, S., DeVinney, R., Bladt, F., Goosney, D., Gelkop, S., Gish, G.D., Pawson, T., and Finlay, B.B. (2001). Enteropathogenic *E. coli* Tir binds Nck to initiate actin pedestal formation in host cells. Nat. Cell Biol. *3*, 856–859.

Higgs, H.N., and Pollard, T.D. (2001). Regulation of actin filament network formation through ARP2/3 complex: activation by a diverse array of proteins. Annu. Rev. Biochem. *70*, 649–676.

Ismaili, A., Philpott, D.J., Dytoc, M.T., and Sherman, P.M. (1995). Signal transduction responses following adhesion of verocytotoxin-producing *Escherichia coli*. Infect. Immun. *63*, 3316–3326.

Kenny, B. (1999). Phosphorylation of tyrosine 474 of the enteropathogenic *Escherichia coli* (EPEC) Tir receptor molecule is essential for actin nucleating activity and is preceded by additional host modifications. Mol. Microbiol. *31*, 1229–1241.

Kenny, B. (2001). The enterohaemorrhagic *Escherichia coli* (serotype O157:H7) Tir molecule is not functionally interchangeable for its enteropathogenic *E. coli* (serotype O127:H6) homologue. Cell. Microbiol. *3*, 499–510.

Kenny, B., DeVinney, R., Stein, M., Reinscheid, D.J., Frey, E.A., and Finlay, B.B. (1997). Enteropathogenic *E. coli* (EPEC) transfers its receptor for intimate adherence into mammalian cells. Cell *91*, 511–520.

Liu, H., Radhakrishnan, P., Magoun, L., Prabu, M., Campellone, K.G., Savage, P., He, F., Schiffer, C.A., and Leong, J.M. (2002). Point mutants of EHEC intimin that diminish Tir recognition and actin pedestal formation highlight a putative Tir binding pocket. Mol. Microbiol. *45*, 1557–1573.

Lommel, S., Benesch, S., Rohde, M., Wehland, J., and Rottner, K. (2004). Enterohaemorrhagic and enteropathogenic *Escherichia coli* use different mechanisms for actin pedestal formation that converge on N-WASP. Cell. Microbiol. *6*, 243–254.

Lommel, S., Benesch, S., Rottner, K., Franz, T., Wehland, J., and Kuhn, R. (2001). Actin pedestal formation by enteropathogenic *Escherichia coli* and intracellular motility of Shigella flexneri are abolished in N-WASP-defective cells. EMBO Rep. *2*, 850–857.

McDaniel, T.K., and Kaper, J.B. (1997). A cloned pathogenicity island from enteropathogenic Escherichia coli confers the attaching and effacing phenotype on *E. coli* K-12. Mol. Microbiol. *23*, 399–407.

McNamara, B.P., Koutsouris, A., O'Connell, C.B., Nougayrede, J.P., Donnenberg, M.S., and Hecht, G. (2001). Translocated EspF protein from enteropathogenic *Escherichia coli* disrupts host intestinal barrier function. J. Clin. Invest. *107*, 621–629.

Murphy, K.C., and Campellone, K.G. (2003). Lambda Red-mediated recombinogenic engineering of enterohemorrhagic and enteropathogenic *E. coli*. BMC Mol. Biol. *4*, 11.

Murphy, K.C., Campellone, K.G., and Poteete, A.R. (2000). PCR-mediated gene replacement in *Escherichia coli*. Gene *246*, 321–330.

Nataro, J.P., and Kaper, J.B. (1998). Diarrheagenic *Escherichia coli*. Clin. Microbiol. Rev. *11*, 142–201.

Perna, N.T., Mayhew, G.F., Posfai, G., Elliott, S., Donnenberg, M.S., Kaper, J.B., and Blattner, F.R. (1998). Molecular evolution of a pathogenicity island from enterohemorrhagic *Escherichia coli* O157:H7. Infect. Immun. *66*, 3810–3817.

Perna, N.T., Plunkett, G., 3rd, Burland, V., Mau, B., Glasner, J.D., Rose, D.J., Mayhew, G.F., Evans, P.S., Gregor, J., Kirkpatrick, H.A., et al. (2001). Genome sequence of enterohaemorrhagic *Escherichia coli* O157:H7. Nature *409*, 529–533.

Rohatgi, R., Nollau, P., Ho, H.-Y.H., Kirschner, M.W., and Mayer, B.J. (2001). Nck and phosphatidylinositol 4,5-bisphosphate synergistically activate actin polymerization through the N-WASP-Arp2/3 pathway. J. Biol. Chem. *276*, 26448–26452.

Viswanathan, V.K., Koutsouris, A., Lukic, S., Pilkinton, M., Simonovic, I., Simonovic, M., and Hecht, G. (2004). Comparative analysis of EspF from enteropathogenic and enterohemorrhagic *Escherichia coli* in alteration of epithelial barrier function. Infect. Immunol. *72*, 3218–3227.

Wagner, P.L., and Waldor, M.K. (2002). Bacteriophage control of bacterial virulence. Infect. Immun. *70*, 3985–3993.

Welch, M.D., and Mullins, R.D. (2002). Cellular control of actin nucleation. Annu. Rev. Cell Dev. Biol. *18*, 247–288.